Please do not adjust margins

Journal Name

ARTICLE

Ring-fused porphyrins: extension of π-conjugation significantly affects the aromaticity and optical properties of the porphyrin π-systems and Lewis acidity of the central metal ions

Received 00th January 20xx,
Accepted 00th January 20xx

DOI: 10.1039/x0xx00000x

www.rsc.org/

Yuta Saegusa,[a] Tomoya Ishizuka,*[a] Keiyu Komamura,[a] Soji Shimizu,[b,¶] Hiroaki Kotani,[a] Nagao Kobayashi[b] and Takahiko Kojima*[a]

Here, we report the effects of the ring fusion, which causes expansion of the π-conjugation circuits of the porphyrin derivatives to the fused *meso*-aryl groups, on the aromaticity and the magnetic properties. These studies revealed the facts that the ring fusion with five-membered rings causes not only the remarkable red shifts of the absorption bands and narrowed HOMO-LUMO gaps, but also the contribution of anti-aromatic resonance forms to the magnetic properties as observed in the ^{1}H NMR spectra. The optical absorption and magnetic circular dichroism (MCD) spectroscopies indicate that the increase in the number of the fused rings causes stabilization of the LUMO level of the porphyrin derivatives and resultantly induces the loosening of the LUMO degeneracy that is generally observed for porphyrins. The electronic structure of a quadruply fused porphyrin derivative was experimentally clarified by the ESR studies on the 1e$^-$-oxidized and 1e$^-$-reduced species in THF. Furthermore, we revealed the substituent effects of the fused *meso*-aryls groups of quadruply fused porphyrins (QFPs) on the crystal structures, absorption spectra and redox potentials; the sensitiveness of the substituent effects is one of the evidences to support that the π-conjugation circuits extended to the fused *meso*-aryl groups. Additionally, the elongation of the bond lengths between the pyrrolic nitrogen and the central metal ions in QFP-metal complexes causes remarkable increase of the Lewis acidity of the central metal ions.

Introduction

Polycyclic aromatic compounds have been extensively studied in relevance to graphite, graphene, fullerenes, and the analogues.[1] In particular, the analogues containing five-membered rings have attracted much attention not only for interests as partial structures of fullerenes[2] but also for interests to the unique aromaticity and the magnetic properties.[3] For instance, pyracylene is a di-etheno-derivative of naphthalene, and it displays a reduced aromatic character due to contribution of the resonance structures involving a 12π anti-aromatic circuit.[4-6]

In recent years, introduction of fused rings on the periphery of the porphyrin aromatic circuit have been intensively studied,[7-16] because of interests on the unique physical properties derived from the narrowed HOMO-LUMO gaps and supramolecular assemblies based on the intermolecular π-π stacking interaction facilitated by the expanded and planar π-conjugation. Due to such unique properties, porphyrins having exocyclic fused rings are considered to be attractive candidates of components to construct photoelectronic devices,[12a,13,14c] molecular wires[11b,16] and so on. Among them, ring-fused porphyrins bearing fused five-membered rings, such as dehydropurpurin, which is an

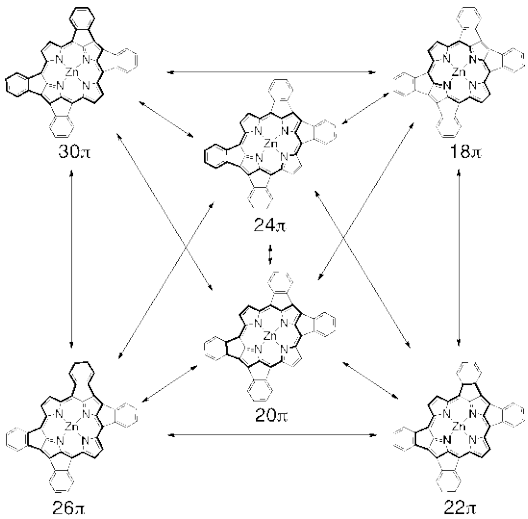

Fig. 1 Resonance structures of ZnQFP (**4**) with aromatic and anti-aromatic circuits.

[a] *Department of Chemistry, Graduate School of Pure and Applied Sciences, University of Tsukuba, 1-1-1 Tennoudai, Tsukuba, Ibaraki 305-8571, Japan. E-mail: ishizuka@chem.tsukuba.ac.jp, kojima@chem.tsukuba.ac.jp; Fax: +81-29-853-4323.*

[b] *Department of Chemistry, Graduate School of Science, Tohoku University, Sendai 980-8578, Japan.*

¶ Present address: *Department of Chemistry and Biochemistry, Graduate School of Engineering, Kyushu University, 744 Motooka, Nishi-Ku, Fukuoka, Fukuoka 819-0395, Japan.*

† Electronic Supplementary Information (ESI) available: Synthetic details, UV-Vis spectral changes in titration experiments, ^{1}H NMR spectra, possible resonance structures of the fused porphyrins, TD-DFT calculations, MCD band patterns, electrochemical data of QFPs. See DOI: 10.1039/x0xx00000x

Please do not adjust margins

Please do not adjust margins

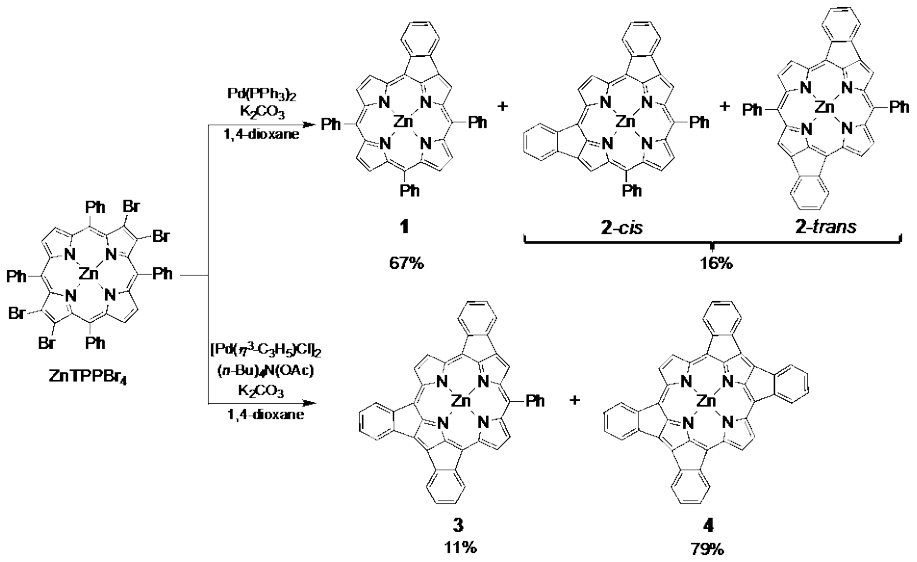

Scheme 1 Syntheses of a series of the ring-fused porphyrin derivatives.

acetylene adduct at the 8 and 10 positions of porphyrin,[17] and the derivatives[18-22] have emerged as a new important class of porphyrinoids and attracted much attention due to the unique optical properties. For instance, dehydropurpurin derivatives have been reported to exhibit relatively shorter lifetimes of the excited states and the resulting weak emissions,[20-22] which derive from the small energy gaps between the frontier orbitals due to the breaking of the degeneracy caused by ring-fusion. Additionally, dehydropurpurin derivatives commonly exhibited red-shifted absorption bands with weak intensity.[18-22]

Recently, we have first reported the synthesis of the zinc(II) complex of a quadruply-fused porphyrin (ZnQFP, **4**), whose exocyclic five-membered fused rings at the periphery exhibit the same bonding pattern as those of dehydropurpurin and the derivatives,[17-22] by intramolecular C-C bond formation through palladium-catalysed C-H activation (Fig. 1).[23] ZnQFP exhibits red-shifted absorption bands and small HOMO-LUMO gaps based on the π-extension by the ring-fusion. However, details of the electronic structure of ZnQFP including the aromaticity and the magnetic properties have yet to be clarified. In this work, we investigate the effect of the number of fused rings on the electronic structures of expanded π-conjugated frameworks derived from the 18π-electron aromatic circuit, by using UV-Vis and MCD spectroscopies. Ring fusion also makes it possible to draw various aromatic circuits including anti-aromatic circuits on the fused porphyrins (Fig. 1 and see below). Spectroscopic results allowed us to confirm considerable effect of the contribution of anti-aromatic circuits on the electronic structures of ZnQFP and the optical absorption properties. Furthermore, we clarify the extension of the aromatic circuits to the fused *meso*-aryl groups using ESR spectroscopies of the $1e^-$-oxidized and $1e^-$-reduced species. Significant substituent effects at the *para*-positions of the fused *meso*-aryl groups of the ZnQFP derivatives have been also clarified on the optical and electrochemical properties and the crystal structures; the sensitiveness to the electronic properties of the substituents are also based on the expansion of the π-conjugated circuits to the fused *meso*-aryl groups. In addition, we confirm the increase of the Lewis acidity of the central metal ions in the QFP ligand, due to elongation of the metal-nitrogen bond lengths caused by rhombic deformation of the rigid structure of the QFP ligand.

Results and discussion

Synthesis

To obtain a series of ring-fused porphyrins, we employed direct C-H activation using a Pd catalyst to link an *o*-carbon of *meso*-aryl groups with a *β*-carbon of *β*-tetrabromo-tetrphenylporphyrin ($TPPBr_4$) (Scheme 1). As previously reported,[23] selection of the Pd catalyst is particularly crucial for the product selectivity of the reaction of $ZnTPPBr_4$. Upon using $Pd^0(PPh_3)_4$ as the catalyst, partially ring-fused porphyrins, **1** and **2**, were mainly formed (Scheme 1; top),[18] where the bromo groups not used for the ring-fusion were eliminated to be replaced with hydrogen atoms. On the other hand, Pd clusters, which were formed from $[Pd(\eta^3\text{-}C_3H_5)Cl]_2$ *in situ*,[24] afforded the fully ring-fused product (**4**) in a high yield (*ca.* 80%) (Scheme 1; bottom).[25]

Herein, to elucidate the impact of the substituents on the electronic characteristics of **4**, we have introduced various functional groups at the *para*-positions of the four *meso*-phenyl groups of the $ZnTPPBr_4$ precursor, $ZnT(Ar)PBr_4$ (Scheme 2). The syntheses of the derivatives were done as follows: The tetra-*meso*-aryl porphyrins were brominated at the four *β*-carbons[26] and the C-C bond formation was performed with Pd clusters derived from $[Pd(\eta^3\text{-}C_3H_5)Cl]_2$ as the catalyst in 1,4-dioxane. The yields of the derivatives are 72% for **5** with *tert*-butyl groups, 65% for **6** with methoxy groups, 22% for **7** with methoxycarbonyl groups and 22% for **8** with trifluoromethyl

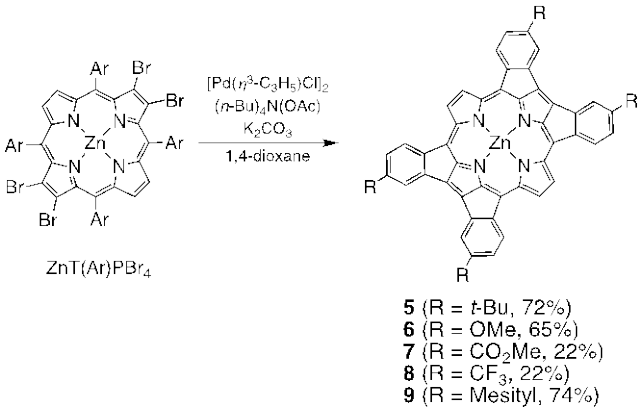

Scheme 2. Syntheses of quadruply fused porphyrin derivatives having substituents at the fused *meso*-aryl groups.

This journal is © The Royal Society of Chemistry 20xx

Please do not adjust margins

Please do not adjust margins

Table 1 NICS(1) values of ZnTPP and the zinc(II) complexes of the fused porphyrins.

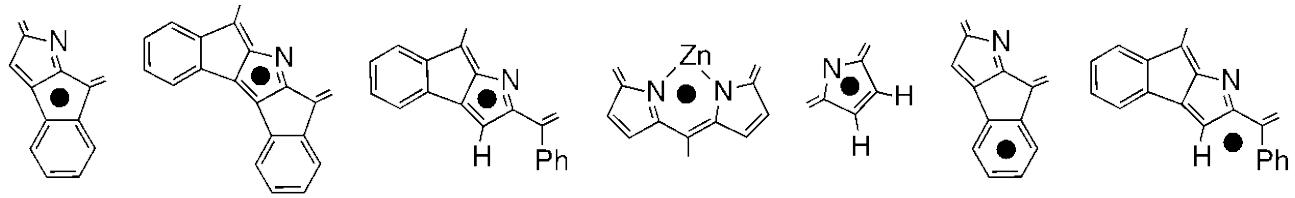

A B C D E F G

	A	B	C	D	E	F	G
ZnTPP	—	—	—	–15.00	–8.56	—	+1.81
1	+12.72	—	–1.24	–12.09[a]	–9.55[a]	–2.81	+1.03
2-*cis*	+9.66	—	–1.81	–9.60[a]	–8.55[a]	–4.01	+0.17
2-*trans*	+11.66	—	–1.16	–10.75[a]	–9.01	–3.19	+0.05
3	+12.37[a]	+6.29	–1.60	–8.59[a]	–7.44[a]	–2.47[a]	–0.53
4	+10.85	+6.21	—	–7.19	–7.33	–3.31	—

[a] Mean values of those for corresponding positions.

groups. The low yields of **7** and **8** are not caused by the low reaction efficiency but by the low solubility of the product and resultant difficulty in isolation. In addition, to improve the solubility of a ZnQFP derivative, mesityl groups were introduced at the *para*-position of the *meso*-aryl groups of ZnT(Ar)PBr_4 to afford **9** in 74% yield. The characterization of the derivatives was done by ^{1}H NMR spectroscopy, MALDI-TOF-MS spectrometry, and elemental analysis.[26]

Partial contribution of anti-aromatic circuits of the fused porphyrins to ^{1}H NMR spectra

In the ^{1}H NMR spectra of **1–4** and ZnTPP in DMSO-d_6, increasing the number of fused rings causes the upfield shifts of the corresponding signals; for instance, ^{1}H NMR signals of protons at β-positions of non-fused pyrroles, adjacent to fused phenyl rings (blue circles in Fig. S1 in the Electronic Supplementary Information (ESI)), were observed at δ 9.31 ppm for **1**, 9.16 ppm for **2**-*cis*, 8.99 ppm for **2**-*trans*, 8.62 ppm for **3** (the mean value of those for the three corresponding signals), and 8.34 ppm for **4**. This tendency seems contrary to the fact that the ring fusion makes the porphyrin molecules more planar and causes π-extension to the fused phenyl groups to generate a larger aromatic circuit. This can be explained by contribution of resonance structures involving anti-aromatic circuits.[20-22] For instance, to quadruply-fused **4**, 30π (4), 26π (8), 22π (4) and 18π (2) aromatic circuits can be drawn (the numbers in parentheses indicate those of the circuit patterns having the number of π-electrons), whereas 24π(4) and 20π (4) anti-aromatic circuits can be expected simultaneously (Fig. S2 in the ESI). In contrast to the aromatic and anti-aromatic circuits expanding to the whole porphyrin molecule, more partial aromatic and anti-aromatic circuits such as 6π benzene rings (4), 8π azapentalene rings (4) and 12π benzo-azapentalene rings (4) can be also drawn. The numbers of possible resonance structures for the other ring-fused porphyrins are summarized in Table S1 in the ESI (See Fig. S3 – S6 in the ESI). These various resonance structures contribute to the magnetic properties of the ring-fused porphyrins depending on the stabilization energy of each resonance structure. In particular, the numbers of anti-aromatic resonance structures increases with increasing the number of the fused rings. This contributes to the up-field shifts of the ^{1}H NMR signals upon increasing the number of the fused rings.

To elucidate the magnetic properties of the ring-fused porphyrins, we have performed DFT calculations on them to estimate nuclear-independent chemical shifts (NICS(1)[27]). The NICS(1) values were estimated on various positions of the ring-fused porphyrins as summarized in Table 1. Negative NICS(1) values indicate diatropic (aromatic) current effects working on the position and the positive values do paratropic (anti-aromatic) current effects. The NICS(1) values for the centres of the six-membered chelate rings of the porphyrin core (position D) and for the centres of the non-fused pyrrole rings (position E) are largely negative commonly for all of the fused porphyrins, indicating the existence of strong aromatic currents in the porphyrin cores. Moreover, the NICS(1) values increased with increasing the number of fused rings. On the other hand, the five-membered rings formed with the ring-fusion exhibit largely positive values at the centres (position A). The positive values at the position A can be accounted for two factors; (1) the five-membered rings are positioned at the outside of the strong aromatic currents of the porphyrin cores, and (2) simultaneously, are involved in the anti-aromatic circuits formed by the ring fusion. In comparison with the NICS(1) values at the outside of the porphyrin aromatic circuits (position G), those at the position A are quite larger and thus the positive values are mainly derived from the anti-aromatic contributions. Additionally, the NICS(1) values at the centres of the fused pyrroles (position B and C) gradually increase with increase in the number of the fused rings, from a negative value for **1** to a positive value for **4**. The tendencies are well

Please do not adjust margins

Please do not adjust margins

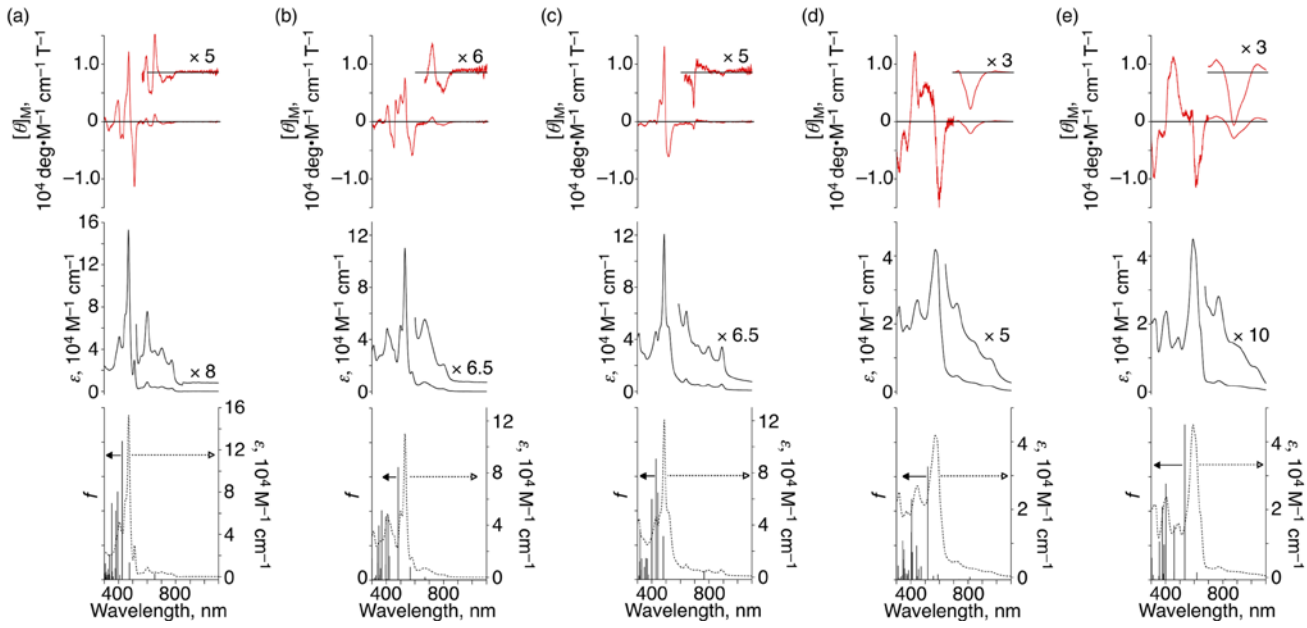

Fig. 2 MCD (top) and experimental absorption (middle) spectra, recorded in DMF at room temperature, and calculated transition energies and oscillator strengths (*f*) obtained with TD-DFT calculations at the B3LYP/6-31G(d) level of theory (bottom) of **1** (a), **2**-*cis* (b), **2**-*trans* (c), **3** (d) and **4** (e). The dashed lines in the calculated stick spectra at the bottom indicate the experimental absorption spectra of the corresponding porphyrins in DMF.

matched with the ^{1}H NMR observations (see above) and well explained with the contribution of the anti-aromatic resonance structures.

Optical spectroscopic characterization of a series of fused porphyrins

The fused porphyrins show the more bathochromically shifted absorption bands with increasing the number of fused rings, indicating the expansion of π-conjugation circuits of the porphyrins (Table S2 in the ESI).[23] The narrowing of the HOMO-LUMO gaps with increasing the number of fused rings was also reflected on the redox potentials of the fused porphyrins and the values obtained by DFT calculations (Table S2 in the ESI); the HOMO-LUMO gaps obtained from the three methods linearly correlated each other (Fig. S7 in the ESI). In addition, the molar coefficients of the absorption bands and the total oscillator strengths decreased with increasing the number of the fused rings. This tendency can be also explained by the contribution of aforementioned anti-aromatic circuits; *i.e.* the anti-aromatic molecules exhibit smaller molar extinction coefficients, because the paratropic character makes the electronic transition spin-forbidden.[28] To rationalize the observed spectral properties, we calculated the electronic absorption spectra with the TD-DFT method at the B3LYP/6-31G(d) level using the DFT-optimized structures of the fused porphyrins. The calculated electronic transition wavelengths and intensities are summarized in Table S3 in the ESI and are schematically depicted in Fig. 2. The calculated stick spectra in Fig. 2 reproduce the excitation wavelengths and intensities of the experimental spectra. The lowest absorption bands of the fused porphyrins commonly derive from the HOMO-to-LUMO π-π* transitions (Fig. S8 and S9 in the ESI).[29]

To gain in-depth insight into the electronic structures of the ring-fused porphyrins based on spectroscopic techniques, their magnetic circular dichroism (MCD) spectra were measured in DMF (Fig. 2).[30–33] Due to the molecular symmetries being lower than C_3, the MCD signals consist of Faraday *B* terms. Despite the less intense and more complicated MCD signal patterns compared to those of regular porphyrins, which can also be accounted for in terms of contributions from other resonance structures to the electronic structures of these compounds, changes in the MCD sign sequence can be observed upon increasing the number of fused rings. In the Q band region, **1** and **2**-*cis* show a negative to positive sign sequence (–, +) in ascending energy, which becomes less intense and unclear for **2**-*trans*, and finally the reverse sign sequence (+, –) was observed for **3** and **4**. According to the Michl's perimeter model for predicting MCD

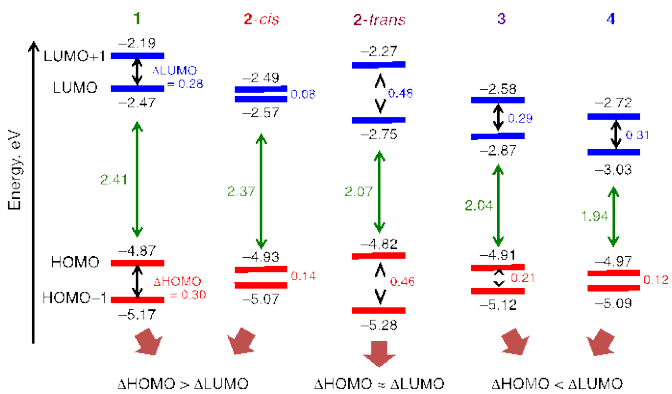

Fig. 3 Illustrations of the MCD band sign patterns predicted by the Michl's perimeter model for the separations of the energy levels of the frontier orbitals obtained for **1** – **4**. Energy levels given in the figure were obtained by DFT calculations at the B3LYP/6-31G(d) level of theory.

This journal is © The Royal Society of Chemistry 20xx

Please do not adjust margins

Please do not adjust margins

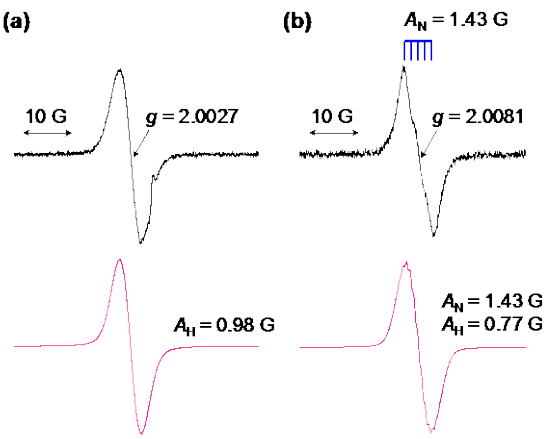

Fig. 4 Experimental (top) and simulated (bottom) ESR spectra of the π-radical cation (a) and anion (b) obtained from the chemical oxidation and reduction of **9** in THF. The former was formed with TBPAH as the oxidant and the latter with $Co(Cp^*)_2$ as the reductant.

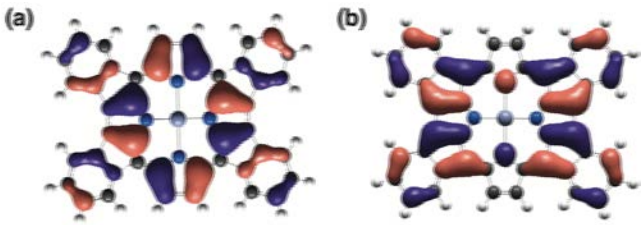

Fig. 5 SOMOs of 1e⁻-oxidized (a) and 1e⁻-reduced species (b) of **4** calculated at the B3LYP/6-31G(d) level of theory.

signs,[30,33] which was successfully applied by Djerassi *et al*. to explain the sign sequence of reduced porphyrins such as chlorin and bacteriochlorin, (–, +) and (+, –) sequences in ascending energy related to the cases of ΔHOMO > ΔLUMO and ΔHOMO < ΔLUMO, respectively (ΔHOMO and ΔLUMO imply the energy gap between HOMO and HOMO–1 and that between LUMO and LUMO+1, respectively).[33,34] It was also demonstrated that in the case of ΔHOMO ≈ ΔLUMO, the MCD signal in the Q band region become (–, –) and basically very weak.[34] By applying this structure-spectrum correlation to the fused porphyrin systems presented here, it can be proposed that the degeneracy of the LUMO and LUMO+1 of the D_{4h} type porphyrin macrocycle is loosened with increasing the number of fused rings, *i.e.* ΔHOMO > ΔLUMO for **1** and **2**-*cis*, ΔHOMO ≈ ΔLUMO for **2**-*trans*, and ΔHOMO < ΔLUMO for **3** and **4** (Fig. 3). In addition, DFT calculations on the fused porphyrins supported well the relative energy changes of the four frontier orbitals and implied that the increase of ΔLUMO is caused by stabilization of the LUMO by the ring fusion (Fig. 3).

Oxidation and reduction of quadruply fused porphyrins

To elucidate the electronic structures of ZnQFP in detail, we measured electron-spin resonance (ESR) spectra of the 1e⁻-oxidized and 1e⁻-reduced species of ZnQFP in THF (Fig. 4). As a ZnQFP derivative, mesityl-substituted **9** was employed for the ESR studies to ensure the solubility in THF and to preclude the association among the radical species. The cyclic and differential-pulse voltammograms (CV and DPV) of **9** measured in THF indicated the rest potential to be +0.13 V vs SCE and exhibited four reversible redox couples at –0.98, –0.60, +0.86, and +1.23 V vs SCE (Fig. S10 in the ESI), and all of the four redox waves was assigned to be 1e⁻ processes. Thus, the first oxidation and reduction potentials of **9** are +0.86 and –0.60 V vs SCE, respectively. The 1e⁻-oxidized species of **9** (**9**•⁺) was formed by addition of 1 equiv of tris(4-bromophenyl)aminium hexachloroantimonate (TBPAH; E_{red} = +1.31 V vs SCE)[35] as the oxidant to the solution of **9** in THF in an ESR tube. The ESR spectrum of **9**•⁺ at 298 K exhibited no hyperfine structure due to the nitrogen nuclei. This result is in stark contrast to that of ZnTPP:[36] The ESR signal of 1e⁻-oxidized ZnTPP in CH_2Cl_2 at 298 K was split into nine lines due to the hyperfine coupling with the four nitrogen nuclei (A_N = 1.55 G). The ESR spectrum of **9**•⁺ was simulated and the signal broadening can be explained by the hyperfine couplings with the peripheral hydrogen nuclei (A_H = 0.98 G).

On the other hand, the ESR signal of 1e⁻-reduced species of **9** (**9**•⁻), which was formed with 1 equiv of decamethylcobaltocene ($Co(Cp^*)_2$; E_{ox} = –1.30 V vs SCE)[37] as a reductant in THF at 222 K, exhibited a five-peaked hyperfine splitting pattern due to coupling with two of the nitrogen nuclei (Fig. 4b). The simulation of the ESR signal was performed to indicate that the hyperfine coupling constants, A_N and A_H, are 1.43 and 0.77 G, respectively. Also in this case, the hyperfine splitting patterns are quite different between the reduced species of ZnQFP and ZnTPP. In the ESR spectrum of 1e⁻-reduced ZnTPP (ZnTPP•⁻) in THF at room temperature, a relatively broadened and isotropic signal was observed without any hyperfine splitting due to the nitrogen nuclei.[38]

The difference in the hyperfine splitting patterns between ZnQFP and ZnTPP can be accounted on the basis of the distribution of the SOMOs obtained by DFT calculations. The SOMO of ZnTPP•⁺ shows a_{2u} symmetry and has a large spin density on the inner four nitrogen atoms,[39] whereas that of ZnQFP•⁺ has a_{1u} symmetry, expanding to the fused phenyl rings, and shows no spin density on the four nitrogen atoms (Fig. 5a). Therefore, the ESR signal of ZnQFP•⁺ does not exhibit hyperfine splitting due to the nitrogen nuclei. On the other hand, calculations of ZnTPP•⁻ exhibits b_{1g} symmetric SOMO having no electron density on the four nitrogen atoms.[40] In contrast, the SOMO of ZnQFP•⁻ in the b_{1g} symmetry possesses electron density on the two nitrogen atoms of the non-fused pyrroles (Fig. 5b). Thus, the ESR signal of ZnQFP•⁻ shows hyperfine splitting due to the two nitrogen nuclei.

Substituent effects on crystal structures of ZnQFP derivatives.

In the previous report,[23] we described the crystal structures of **4**-py (the molecule written after hyphen indicates the axial ligand on the central Zn^{II} ion). Here, we have clarified crystal structures of QFP derivatives, **5**-py, **5**-dox (dox = 1,4-dioxane) and **8**-py (Fig. 6).[26] The representative bond lengths and other structural parameters of the crystal structures are summarized in Table 2. One of the most important structural characteristics of QFP is the elongation of the C_{ipso}-C_{ortho} bonds of the fused rings; the elongation derives from the expansion of the π-conjugation circuits to the fused benzene rings.[23] As results of

Please do not adjust margins

Please do not adjust margins

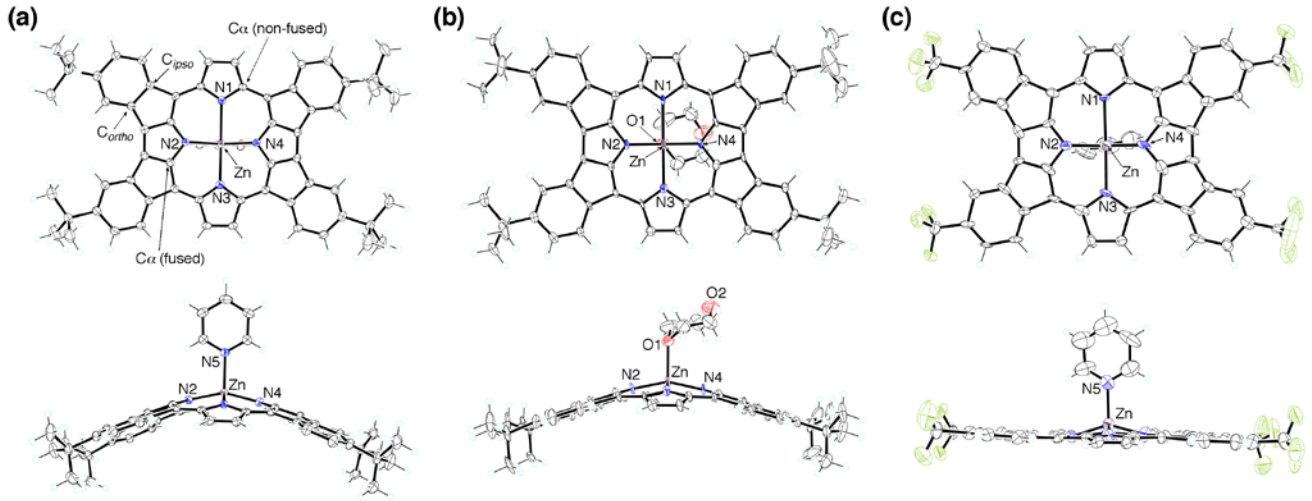

Fig. 6 Top and side views of crystal structures of **5**-py (a), **5**-dox (b) and **8**-py (c). The thermal ellipsoids are drawn with 50% probability. Green-coloured atoms in (c) indicate fluorine atoms.

the expansion, not only 18π□ □□□□

Please do not adjust margins

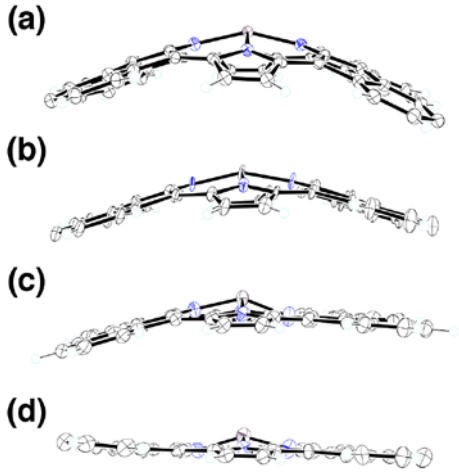

Fig. 7 Side views of porphyrin cores consisting of 48 atoms of **5**-py (a), **5**-dox (b), **4**-py (c) and 8-py (d). The thermal ellipsoids are drawn with 50% probability. The axial ligands and the substituents at the para-positions are omitted for clarity.

although the reason for this tendency is not clear at this point. The bond lengths are very similar among **4**-py, **5**-X and **8**-py as mentioned above and only the difference was found in the atom distance between the nitrogen atoms of the fused pyrrole ring (N2···N4) (Table 2). Therefore, the substituents at the fused phenyl rings do not affect the size of the porphyrin core so significantly.

Substituent effects on optical and electrochemical properties of quadruply fused porphyrins.

The optical and electrochemical properties of ZnQFP are largely affected by the substituents at the *para*-position of the fused *meso*-aryl groups. The introduction of substituents at the *para*-positions of the fused aryl groups caused bathochromic shifts of the absorption bands for all of the four derivatives, **5**–**9**, relative to those of **4** (Table 3 and Fig. S11 in the ESI). Comparing the shift widths in an energy unit (cm^{-1}) with those of ZnTPP and the derivatives, the absorption bands of ZnQFP derivatives are 10 times more affected by the substituents than those of ZnTPP; for instance, the methoxy-substituted ZnQFP, **6**, exhibits the longest Q-band at 1200 nm (8330 cm^{-1}) in DMF and the shift width relative to that of **4** is 1460 cm^{-1}, whereas the shift width of the Q-band for ZnT(*p*-OMe)PP to that of ZnTPP is only 110 cm^{-1}.

As mentioned above, the absorption bands of the ZnQFP derivatives are highly affected by the *meso*-aryl substituents, whereas the direction and width of the shifts is not correlated with the electronic properties of the substituents: Both the electron-withdrawing and -donating groups cause red shifts of the absorption bands. To shed light on the substituent effects for the perturbation of the energy levels of the frontier orbitals that most directly relate to the π-π* transitions,[43] we performed electrochemical studies on the ZnQFP derivatives to determine the redox potentials of the ZnQFP and ZnTPP derivatives (Fig. S12 in the ESI). The redox potentials are also summarized in Table 3. Both of the potentials for the first reduction and first oxidation processes, E_{Red1} and E_{Ox1}, of the ZnQFP derivatives were positively shifted upon introducing electron-withdrawing groups (Fig. 8). E_{Ox1} of the ZnQFP derivatives is more sensitive to the substituents than E_{Red1}; the differences in the potentials between the most electron-donating methoxy derivative, **6**, and the most electron-withdrawing trifluoromethyl one, **8**, are 0.51 V for E_{Ox1} (+0.37 V for **6** and +0.88 V for **8**), whereas that for E_{Red1} is only 0.05 V

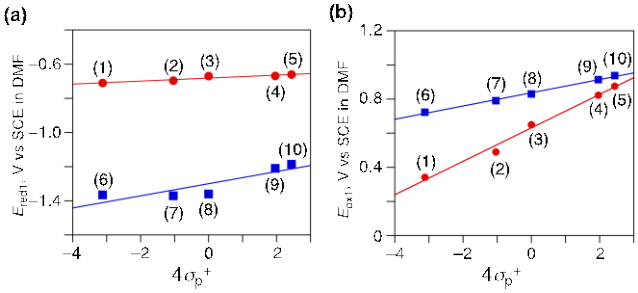

Fig. 8 Hammett plots of E_{Red1} (a) and E_{Ox1} (b) of the ZnQFP and ZnTPP derivatives ((1): **6**, (2): **5**, (3): **4**, (4): **7**, (5): **8**, (6): ZnT(*p*-OMe)PP, (7): ZnT(*p*-*t*Bu)PP, (8): ZnTPP, (9): ZnT(*p*-CO_2Me)PP, (10): ZnT(*p*-CF_3)PP) against $4\sigma_p^+$. Solvent: DMF containing 0.1 M $TBAPF_6$ (TBA = tetra(*n*-butyl)ammonium). Values of σ_p^+ are taken from ref. 43.

Table 3 Absorption maxima and redox potentials of QFP and ZnTPP derivatives in DMF.

	λ_{max}(B)[a]	ν(B)[b]	$\Delta\nu$(B)[b]	λ_{max}(Q)[a]	ν(Q)[b]	$\Delta\nu$(Q)[b]	E_{Red1}[c]	E_{Ox1}[c]	E_{Ox1}–E_{Red1}[d]
4 (R = H)	592	16900	—	1021	9790	—	−0.67	+0.65	1.32
5 (R = *t*-Bu)	616	16230	−670	1060	9430	−360	−0.70	+0.49	1.19
6 (R = OMe)	637	15700	−1200	1200	8330	−1460	−0.71	+0.37	1.08
7 (R = CO_2Me)	616	16230	−670	1046	9560	−230	−0.67	+0.82	1.49
8 (R = CF_3)	598	16840	−60	1104	9060	−730	−0.66	+0.88	1.54
ZnTPP	425	23530	0	599	16690	0	−1.36	+0.83	2.19
ZnT(*p*-*t*Bu)PP	427	23420	−110	601	16640	−50	−1.37	+0.79	2.16
ZnT(*p*-OMe)PP	429	23310	−220	603	16580	−110	−1.36	+0.74	2.10
ZnT(*p*-CO_2Me)PP	429	23310	−220	600	16660	−30	−1.21	+0.91	2.12
ZnT(*p*-CF_3)PP	426	23470	−60	597	16750	60	−1.19	+0.94	2.13

[a] in nm. [b] in cm^{-1}. [c] in V vs SCE. [d] in V.

Please do not adjust margins

Please do not adjust margins

(–0.71 V for **6** and –0.66 V for **8**). On the other hand, the redox potentials of the ZnTPP derivatives are less sensitive to the substituents of the *meso*-phenyl groups. To confirm this tendency in the substituent effects on the redox potentials, we provided Hammett plots (Fig. 8). A Hammett parameter, σ_p^+,[44] was the best fit for the present studies. Consequently, the plots of the redox potentials against σ_p^+ exhibited good linearity and the coefficients, ρ, were obtained to be +0.098 and +0.009 for E_{Ox1} and E_{Red1} of ZnQFPs, respectively, and +0.039 and +0.035 for E_{Ox1} and E_{Red1} of ZnTPPs, respectively. As indicated by the ρ values, E_{Ox1} of ZnQFP is sensitive to the substituents than the E_{Red1}, and the redox potentials of ZnQFP are more easily affected by the substituents than those of ZnTPP.[45] This sensitiveness can be accounted by the distribution of the electron densities in the frontier orbitals (Fig. 9). The DFT-calculated HOMO and LUMO show large distribution on the *meso*-aryl groups due to the ring-fusion and resultant expansion of the π-conjugation. In particular, the *para*-position of the fused *meso*-aryl groups has large electron density in the HOMO, but no distribution of the LUMO, which causes good sensitivity of the HOMO-related E_{Ox1} and poor sensitivity of LUMO-related E_{Red1} to the substituents.

Lewis acidity of the central Zn^{II} ion in QFP

One of the structural characteristics of ZnQFP complexes is the rhombic distortion around the Zn^{II} centers;[23] that is, the Zn–N distances for the nitrogen atoms of the fused pyrroles (Zn–N2 and Zn–N4) are shorter by *ca*. 0.27 Å than those of the non-fused pyrroles (Zn–N1 and Zn–N3) and the mean Zn-N distance of the ZnQFP complexes (*ca.* 2.11 Å) is longer than that of ZnTPP (*ca.* 2.04 Å).[46,47] This remarkable elongation suggests weak overall σ-donation from the nitrogen atoms of the QFP ligand to the central Zn^{II} ion. This overall elongation of Zn-N bonds is expected to enhance the Lewis acidity of the central Zn^{II} ion. To confirm the enhancement of the Lewis acidity, we

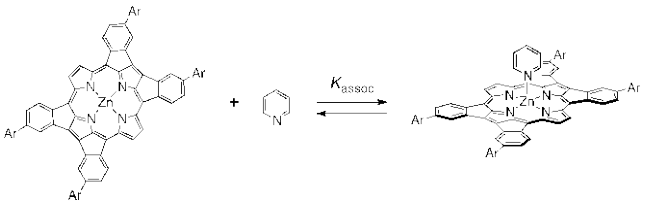

Scheme 3 Coordination of pyridine on the Zn center of a QFP derivative.

Table 4. Association constants of **9** and other Zn^{II} complexes of porphyrin derivatives with pyridine derivatives in CH_2Cl_2 at 298 K.

	K_{assoc}, M^{-1}, 10^4 M^{-1}					
	py		3-Am-py		4-Me-py	
9	76	□5	38	□7	30	□1
ZnTPP	1.1	[b]□0.	1.8	[b]□0.	1.10	□
ZnOPP[a]	1.4	[b]□0.	3.2	[b]□0.	3.5	□0
ZnDPP	4.6	[b]□0.	11	[b]□0	7.5	□0

[a] OPP = 2,3,5,10,12,13,15,20-octaphenylporphyrin, [b] ref. 48c.

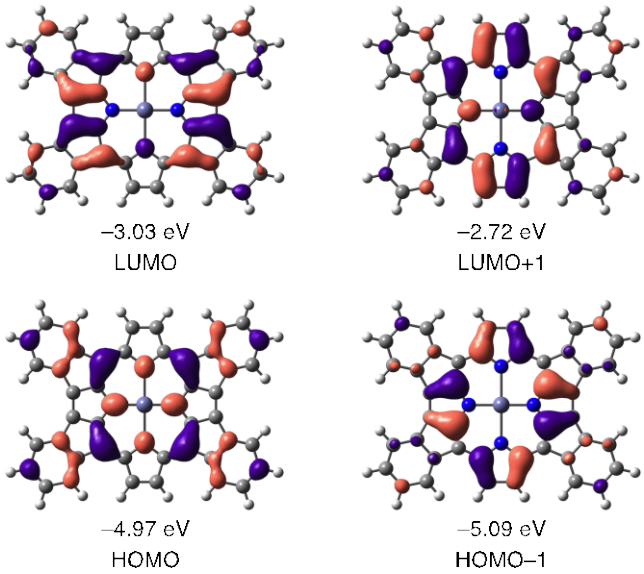

Fig. 9 The frontier orbitals of **4** calculated at the B3LYP/6-31G(d) level of theory.

have determined the association constants (K_{assoc}) between a ZnQFP derivative, **9**, and pyridine derivatives in CH_2Cl_2 (Scheme 3). Here, we utilized three pyridine derivatives, pyridine (py), 3-aminopyridine (3-Am-py), and 4-methylpyridine (4-Me-py). The solution of each pyridine derivative in CH_2Cl_2 was added dropwise to that of **9** (1.26×10^{-5} M) in CH_2Cl_2 and the UV-Vis spectral change was observed (Fig. S13 in the ESI) at 298 K. The absorbance changes of **9** at 625 nm upon the titration experiments were analysed with eq S1 in the ESI to afford the K_{assoc} values, which are summarized in Table 4. In comparison with the K_{assoc} values of Zn^{II} complexes of other porphyrin derivatives (Fig. S14 in the ESI), compound **9** exhibits larger K_{assoc} values for all of the three pyridine derivatives. For instance, the K_{assoc} of **9** for py ($(7.6 \pm 0.5) \times 10^5$ M^{-1}) is *ca.* 70 times larger than that of ZnTPP ($(1.1 \pm 0.1) \times 10^4$ M^{-1})[48] and *ca.* 16 times larger than even that of the Zn^{II} complex of dodecaphenylporphyrin (DPP), which has been known to exhibit relatively higher Lewis acidity due to the conformational distortion to a saddle form and the resulting weak σ-donation from the nitrogen atoms to the central metal ions.[48c] Therefore, the structural expansion of the core of the QFP ligand can exert remarkable impact to enhance the Lewis acidity of the central metal ions.

Conclusions

We have clarified the significant effects of the ring fusion on the electronic structures of the porphyrin derivatives, and verified the expansion of the π-conjugated aromatic circuits to the fused *meso*-aryl groups. The expansion of the π-conjugated circuits results in the unique aromatic and magnetic properties of the porphyrin derivatives, and causes not only the remarkable red shifts of the absorption bands derived from narrowed HOMO-LUMO gaps, but also the contribution of anti-aromatic resonance forms to the magnetic properties as observed in the ^{1}H NMR spectra. In addition, we

This journal is © The Royal Society of Chemistry 20xx

Please do not adjust margins

Please do not adjust margins

have revealed the substituent effects at the fused *meso*-aryl groups of QFP on the crystal structures, absorption spectra and redox potentials; the significant substituent effects are also caused by the expansion of the π-conjugated circuits. Furthermore, the ring fusion to form five-membered rings causes overall elongation of the coordination bonds among the pyrrolic nitrogen atoms and the central metal ions in QFP-metal complexes, which results in remarkable enhancement of the Lewis acidity of the central metal ions to strengthen the axial coordination.

Experimental section

General.

Chemicals and solvents were used as received from commercial sources unless otherwise mentioned. 1,4-dioxane for the synthesis was distilled over Na/benzophenone before use. *N*,*N*-Dimethylfolmamide (DMF) for the electrochemical measurements was distilled before use. Synthesis of Zn^{II} tetrabromo-porphyrinate derivatives,[49] **1**, **2**-*cis*, **3**, and **4**,[23] were performed with the reported procedures. Synthetic details of compounds are described in the ESI.

^{1}H NMR measurements were performed on a Bruker AVANCE400 spectrometer at 400 MHz. UV-vis absorption spectra were measured at room temperature in DMF on a Shimadzu UV-3600 spectrophotometer. MALDI-TOF-MS spectrometry was performed on an AB SCIEX TOF/TOF 5800 spectrometer by using dithranol as a matrix. Magnetic circular dichroism (MCD) spectra in the 300-800 nm region were recorded on a JASCO J-725 spectrodichrometer with a magnetic field of up to 1.09 T, while spectra in the 800-1200 nm region were recorded using a JASCO J-730 spectrodichrometer producing a magnetic field of up to 1.50 T (1 T = 1 tesla). Electrochemical measurements were performed at room temperature in THF and DMF in the presence of 0.1 M of $TBAPF_6$ as an electrolyte at room temperature on an ALS/CH Instruments Electrochemical Analyser Model 710D. ESR spectroscopy was performed on a Bruker EMXPlus9.5/2.7 spectrometer.

Acknowledgements

The authors thank Dr. Atsuya Muranaka at RIKEN, Prof. Masanobu Uchiyama at the University of Tokyo, and Dr. Taniyuki Furuyama at Tohoku University for near IR MCD measurements. This work was supported by Grants-in-Aid (Nos. 22750118, 25410033 and 24245011) from Japan Society for the Promotion of Science (JSPS).

Notes and references

1 (a) A. Sygula and P. W. Rabideau, *Carbon-Rich Compounds: From Molecules to Materials*, M. M. Haley and R. R. Tykwinski, Eds.; Wiley-VCH: Weinheim, 2006; (b) C. Li, M. Liu, N. G. Pschirer, M. Baumgarten, K. Müllen, *Chem. Rev.*, 2010, **110**, 6817; (c) K. K. Baldridge and J. S. Siegel, *Angew. Chem., Int. Ed.* 2013, **52**, 5436; (d) C. Thilgen and F. Diederich, *Chem. Rev.* 2006, **106**, 5049.

2 (a) L. T. Scott, *Angew. Chem., Int. Ed.*, 2004, **43**, 4994; (b) Y.-T. Wu and J. S. Siegel, *Chem. Rev.*, 2006, **106**, 4843; (c) V. M. Tsefrikas and L. T. Scott, *Chem. Rev.*, 2006, **106**, 4868; (d) S. Higashibayashi and H. Sakurai, *Chem. Lett.*, 2011, **40**, 122; (e) L. T. Scott, M. M. Boorum, B. J. McMahon, S. Hagen, J. Mack, J. Blank, H. Wegner and A. de Meijere, *Science*, 2002, **295**, 1500.

3 (a) Z. Chen and R. B. King, *Chem. Rev.*, *2005*, **105**, 3613; (b) X. Lu, Z. Chen, *Chem. Rev.*, 2005, **105**, 3643. (c) G. A. Burley, *Angew. Chem., Int. Ed.*, 2005, **44**, 3176.

4 (a) B. M. Trost and G. M. Bright, *J. Am. Chem. Soc.*, 1967, **89**, 4244; (b) B. M. Trost, G. M. Bright, C. Frihart and D. Britteli, *J. Am. Chem. Soc.*, 1971, **93**, 737.

5 (a) B. Freiermuth, S. Gerber, A. Riesen, J. Wirz and M. Zehnder, *J. Am. Chem. Soc.*, 1990, **112**, 738; (b) H. P. Diogo, T. Kiyobayashi, M. E. Minas da Piedade, N. Burlak, D. W. Rogers, D. McMasters, G. Persy, J. Wirz and J. F. Liebman, *J. Am. Chem. Soc.*, 2002, **124**, 2065; (c) M. Randic, *Chem. Rev.*, 2003, **103**, 3449; (d) E. Steiner and P. W. Fowler, *J. Phys. Chem. A*, 2001, **105**, 9553.

6 (a) H. A. Wegner, H. Reisch, K. Rauch, A. Demeter, K. A. Zachariasse, A. de Meijere and L. T. Scott, *J. Org. Chem.*, 2006, **71**, 9080; (b) R. W. Havenith, H. Jiao, L. W. Jenneskens, J. H. van Lenthe, M. Sarobe, P. von Ragué Schleyer, M. Kataoka, A. Necula and L. T. Scott, *J. Am. Chem. Soc.*, 2002, **124**, 2363.

7 Reviews on this topic: (a) S. Fox and R. W. Boyle, *Tetrahedron*, 2006, **62**, 10039; (b) J. P. Lewtak and D. T. Gryko, *Chem. Commun.*, 2012, **48**, 10069; (c) H. Mori, T. Tanaka and A. Osuka, *J. Mater. Chem. C*, 2013, **1**, 2500.

8 (a) L. Edwards, M. Gouterman and C. B. Rose, *J. Am. Chem. Soc.*, 1976, **98**, 7638; (b) T. D. Lash and B. H. Novak, *Angew. Chem., Int. Ed. Engl.*, 1995, **34**, 683; (c) S. Ito, T. Murashima, H. Uno and N. Ono, *Chem. Commun.*, 1998, 1661.

9 (a) R. Deshpande, L. Jiang, G. Schmidt, J. Rakovan, X. Wang, K. Wheeler and H. Wang, *Org. Lett.*, 2009, **11**, 4251; (b) L. Jinag, J. T. Engle, L. Sirk, C. S. Hartley, C. J. Ziegler and H. Wang, *Org. Lett.*, 2011, **13**, 3020; (c) S. Banala, T. Rühl, K. Wurst and B. Kräutler, *Angew. Chem., Int. Ed.*, 2009, **48**, 599.

10 (a) H. Aihara, L. Jaquinod, D. J. Nurco and K. M. Smith, *Angew. Chem., Int. Ed.*, 2001, **40**, 3439; (b) M. Nath, J. C. Huffman and J. M. Zaleski, *J. Am. Chem. Soc.*, 2003, **125**, 11484; (c) M. Nath, M. Pink and J. M. Zaleski, *J. Am. Chem. Soc.*, 2005, **127**, 478.

11 (a) A. N. Cammidge, P. J. Scaife, G. Berber, D. L. Hughes, *Org. Lett.*, 2005, **7**, 3413; (b) M. Tanaka, S. Hayashi, S. Eu, T. Umeyama, Y. Matano and H. Imahori, *Chem. Commun.*, 2007, 2069; (c) C. Jiao, K.-W. Huang, Z. Guan, Q.-H. Xu and J. Wu, *Org. Lett.*, 2010, **12**, 4046.

12 (a) H. S. Gill, M. Harmjanz, J. Santamaría, I. Finger and M. J. Scott, *Angew. Chem., Int. Ed.*, 2004, **43**, 485; (b) K. Kurotobi, K. S. Kim, S. B. Noh, D. Kim and A. Osuka, *Angew. Chem., Int. Ed.*, 2006, **45**, 3944.

13 C. Jiao, L. Zhu and J. Wu, *Chem.–Eur. J.*, 2011, **17**, 6610.

14 (a) N. K. S. Davis, M. Pawlicki and H. L. Anderson, *Org. Lett.*, 2008, **10**, 3945; (b) N. K. S. Davis, A. L. Thompson and H. L. Anderson, *Org. Lett.*, 2010, **12**, 2124; (c) N. K. S. Davis, A. L. Thompson and H. L. Anderson, *J. Am. Chem. Soc.*, 2011, **133**, 30.

15 (a) K. Sendt, L. A. Johnston, W. A. Hough, M. J. Crossley, N. S. Hush and J. R. Reimers, *J. Am. Chem. Soc.*, 2002, **124**, 9299; (b) R. Paolesse, L. Jaquinod, F. S. Della, D. J. Nurco, L. Prodi, M. Montalti, C. D. Natale, A. D'Amico, A. D. Carlo, P. Lugli and K. M. Smith, *J. Am. Chem. Soc.*, 2000, **122**, 11295; (c) H. Uno, A. Masumoto and N. Ono, *J. Am. Chem. Soc.*, 2003, **125**,

Please do not adjust margins

Please do not adjust margins

12082; (d) M. Akita, S. Hiroto and H. Shinokubo, *Angew. Chem., Int. Ed.*, 2012, **51**, 2894.

16 (a) A. Tsuda, A. Nakano, H. Furuta, H. Yamochi and A. Osuka, *Angew. Chem., Int. Ed.*, *2000*, **39**, 558; (b) A. Tsuda, H. Furuta and A. Osuka, *Angew. Chem., Int. Ed.*, 2000, **39**, 2549; (c) A. Tsuda, H. Furuta and A. Osuka, *J. Am. Chem. Soc.*, 2001, **123**, 10304; (d) A. Tsuda and A. Osuka, *Science*, 2001, **293**, 79; (d) Y. Nakamura, N. Aratani, H. Shinokubo, A. Takagi, T. Kawai, T. Matsumoto, Z. S. Yoon, D. Y. Kim, T. K. Ahn, D. Kim, A. Muranaka, N. Kobayashi and A. Osuka, *J. Am. Chem. Soc.*, 2006, **128**, 4119.

17 (a) R. B. Woodward, W. A. Ayer, J. M. Beaton, F. Bickelhaupt, R. Bonnet, P. Buchschacher, G. L. Closs, H. Dutler, J. Hannah, F. P. Hauck, S. Ito, A. Langemann, E. Le Goff, W. Leimgruber, W. Lwowski, J. Sauer, Z. Valenta and H. Volz, *J. Am. Chem. Soc.*, 1960, **82**, 3800; (b) R. B. Woodward, W. A. Ayer, J. M. Beaton, F. Bickelhaupt, R. Bonnet, P. Buchschacher, G. L. Closs, H. Dutler, J. Hannah, F. P. Hauck, S. Ito, A. Langemann, E. Le Goff, W. Leimgruber, W. Lwowski, J. Sauer, Z. Valenta and H. Volz, *Tetrahedron*, 1990, **46**, 7599.

18 (a) S. Fox and R. W. Boyle, *Chem. Commun.*, 2004, 1322. (b) D.-M. Shen, C. Liu and Q.-Y. Chen, *Chem. Commun.*, 2005, 4982; (c) D.-M. Shen, C. Liu and Q.-Y. Chen, *J. Org. Chem.*, 2006, **71**, 6508.

19 (a) S. Hayashi, Y. Matsubara, S. Eu, H. Hayashi, T. Umeyama, Y. Matano and H. Imahori, *Chem. Lett.*, 2008, **37**, 846; (b) T. D. Lash, B. E. Smith, M. J. Melquist and B. A. Godfrey, *J. Org. Chem.*, 2011, **76**, 5335; (c) A. M. V. M. Pereira, M. G. P. M. S. Neves, J. A. S. Cavaleiro, C. Jeandon, J.-P. Gisselbrecht, S. Choua and R. Ruppert, *Org. Lett.*, 2011, **13**, 4742.

20 (a) Y. Mitsushige, S. Yamaguchi, B. S. Lee, Y. M. Sung, S. Kuhri, C. A. Schierl, D. M. Guldi, D. Kim and Y. Matsuo, *J. Am. Chem. Soc.*, 2012, **134**, 16540; (b) H. Fliegl, N. Özcan, R. Mera-Adasme, F. Pichierri, J. Jusélius and D. Sundholm, *Mol. Phys.*, 2013, **111**, 1364.

21 (a) A. Nakano, N. Aratani, H. Furuta and A. Osuka, *Chem. Commun.*, 2001, 1920; (b) A. K. Sahoo, S. Mori, H. Shinokubo and A. Osuka, *Angew. Chem., Int. Ed.*, 2006, **45**, 7972; (c) N. Fukui, H. Yorimitsu, J. M. Lim, D. Kim and A. Osuka, *Angew. Chem., Int. Ed.*, 2014, **53**, 4395.

22 (a) N. Fukui, W.-Y. Cha, S. Lee, S. Tokuji, D. Kim, H. Yorimitsu and A. Osuka, *Angew. Chem., Int. Ed.*, 2013, **52**, 9728; (b) K. Ota, T. Tanaka and A. Osuka, *Org. Lett.*, 2014, **16**, 2974.

23 T. Ishizuka, Y. Saegusa, Y. Shiota, K. Ohtake, K. Yoshizawa and T. Kojima, *Chem. Commun.*, 2013, **49**, 5939.

24 S. Higashibayashi and H. Sakurai, *Chem. Lett.*, 2007, **36**, 18.

25 In the previous report (ref. 23), we described synthesis and characterization of a series of fused porphyrins, singly-fused (**1**), *cis*-doubly-fused (**2**-*cis*), triply-fused (**3**) and quadruply-fused (**4**) porphyrins. Here, we also succeeded in isolation of *trans*-doubly fused porphyrin (**2**-*trans*) (See the ESI). The doubly-fused porphyrins obtained in this work include three isomers; 7,22-&18,40-fused, **2**-*cis*, 7,22-&17,34-fused, **2**-*trans*, and 7,22-&8,28-fused, **2'**-*cis* (see ref. 23). **2'**-*cis* was a very minor product under the reaction conditions and difficult to be isolated.

26 See the ESI.

27 The symbol of (1) represents that the NICS values are estimated at 1 Å above from the π-conjugated planes: (a) P. von Ragué Schleyer, C. Maerker, A. Dransfeld, H. Jiao and N. J. R. van Eikema Hommes, *J. Am. Chem. Soc.*, 1996, **118**, 6317. (b) J. A. N. F. Gomes and R. B. Mallion, *Chem. Rev.*, 2001, **101**, 1349.

28 (a) T. Ito, Y. Hayashi, S. Shimizu, J.-Y. Shin, N. Kobayashi and H. Shinokubo, *Angew. Chem., Int. Ed.*, 2012, **51**, 8542; (b) S. Mori and A. Osuka, *J. Am. Chem. Soc.*, 2005, **127**, 8030.

29 As shown in Table S3 in the ESI, the main contribution to the lowest-energy absorption band stems from the HOMO-to-LUMO π-π* transition commonly for all the ring-fused porphyrins; however, other π-π* transitions also contribute to the lowest-energy absorptions of the fused porphyrins as minor components.

30 (a) J. Michl, *J. Am. Chem. Soc.*, 1978, **100**, 6801; (b) A. Ceulemans, W. Oldenhof, C. Gorller-Walrand and L. G. Vanquickenborne, *J. Am. Chem. Soc.*, 1986, **108**, 1155.

31 (a) J. Mack, M. J. Stillman and N. Kobayashi, *Coord. Chem. Rev.*, 2007, **251**, 429; (b) J. Mack and M. J. Stillman, *Coord. Chem. Rev.*, 2001, **219-221**, 993.

32 (a) A. Muranaka, M. Yokoyama, Y. Matsumoto, M. Uchiyama, A. Tsuda, A. Osuka and N. Kobayashi, *ChemPhysChem*, 2005, **6**, 171; (b) J. Mack, Y. Asano, N. Kobayashi and M. J. Stillman, *J. Am. Chem. Soc.*, 2005, **127**, 17697; (c) S. Sripothongnak, C. J. Ziegler, M. R. Dahlby and V. N. Nemykin, *Inorg. Chem.*, **2011**, ***50***, 6902.

33 (a) J. Michl, *J. Am. Chem. Soc.*, 1978, **100**, 6812; (b) J. Michl, *J. Am. Chem. Soc.*, 1978, **100**, 6819; (c) J. Michl, *Pure Appl. Chem.*, 1980, **52**, 1549.

34 J. D. Keegan, A. M. Stolzenberg, Y.-C. Lu, R. E. Linder, G. Barth, A. Moscowitz, E. Bunnenberg and C. Djerassi, *J. Am. Chem. Soc.*, 1982, **104**, 4317.

35 The reduction potential of TBPAH was determined by cyclic voltammograms in THF containing 0.1 M $TBAPF_6$ as an electrolyte at 298 K.

36 K. Ichimori, H. Ohya-Nishiguchi and N. Hirota, *Bull. Chem. Soc. Jpn.*, 1988, **61**, 2753.

37 J. Ruiz and D. *C.* Astruc, *R. Acad. Sci. Paris, Chimie* 1998, **1**, 21.

38 (a) R. H. Felton and H. Linschitz, *J. Am. Chem. Soc.*, 1966, **88**, 1113; (b) G. L. Closs and L. E. Closs, *J. Am. Chem. Soc.*, 1963, **85**, 818; (c) J. Seth and D. F. Bocian, *J. Am. Chem. Soc.*, 1994, **116**, 143; (d) J. Pawlik, G. Lileta, S. Karabunarliev and M. Baugmgarten, *Chem. Phys.*, 1997, **221**, 121.

39 T. Vangberg, R. Lie and A. Ghosh, *J. Am. Chem. Soc.*, 2002, **124**, 8122.

40 K. Yoshizawa, T. Nakayama, T. Kamachi and P. M. Kozlowski, *J. Phys. Chem. A*, 2007, **111**, 852.

41 Typical C-C bond lengths of phenyl rings are *ca.* 1.38 Å for porphyrin derivatives: (a) C. K. Schauer, O. P. Anderson, S. S. Eaton, G. R. Eaton, *Inorg. Chem.*, 1985, **24**, 4082; (b) M. P. Byrn, C. J. Curtis, I. Goldberg, Y. Hsiou, S. I. Khan, P. A. Sawin, S. K. Tendick, C. E. Strouse, *J. Am. Chem. Soc.*, 1991, **113**, 6549; (c) E. B. Fleischer, C. K. Miller, L. E. Webb, *J. Am. Chem. Soc.*, 1964, **86**, 2342; (d) W. R. Scheidt, J. U. Mondal, C. W. Eigenbrot, A. Adler, L. J. Radonovich, J. L. Hoard, *Inorg. Chem.*, 1986, **25**, 795.

42 (a) D. J. Nurco, C. J. Medforth, T. P. Forsyth, M. M. Olmstead and K. M. Smith, *J. Am. Chem. Soc.*, 1996, **118**, 10918; (b) C. J. Medforth, M. O. Senge, K. M. Smith, L. D. Sparks, and J. A. Shelnutt, *J. Am. Chem. Soc.* 1992, **114**, 9859.

43 (a) A. D. Bond, N. Feeder, J. E. Redman, S. J. Teat and J. K. M. Sanders, *Crystal Growth Des.*, 2002, **2**, 27; (b) Y. Inokuma, Z. S. Yoon, D. Kim and A. Osuka, *J. Am. Chem. Soc.*, 2007, **129**, 4747.

44 C. Hansch, A. Leo and R. W. Taft, *Chem. Rev.*, 1991, **91**, 165.

45 Similar sensitiveness to the substituents has been also reported to the redox potentials of TPP derivatives with the *β*-substituents. (a) A. Giraudeau, H. J. Callot and M. Gross, *Inorg. Chem.*, 1979, **18**, 201; (b) K. M. Kadish and M. M. Morrison, *J. Am. Chem. Soc.*, 1976, **98**, 3326.

46 M. P. Byrn, C. J. Curtis, Y. Hsiou, S. I. Khan, P. A. Sawin, S. K. Tendick, A. Terzis and C. E. Strouse, *J. Am. Chem. Soc.*, 1993, **115**, 9480.

47 Rhombic distortions were also found in other porphyrin derivatives. (a) A. N. Kozyrev, V. Suresh, S. Das, M. O. Senge, M. Shibata, T. J. Dougherty and R. K. Pandey, *Tetrahedron* 2000, **56**, 3353; (b) M. O. Senge, W. W. Kalisch and S. Runge, *Tetrahedron* 1998, **54**, 3781; (c) M. O. Senge, Y. M. Shaker, M.

This journal is © The Royal Society of Chemistry 20xx

Please do not adjust margins

Please do not adjust margins

Pintea, C. Ryppa, S. S. Hatscher, A. Ryan and Y. Sergeeva, *Eur. J. Org. Chem.* 2010, 237.
48 (a) C. H. Kirksey, P. Hambright and C. B. Storm, *Inorg. Chem.* 1969, **8**, 2141; (b) T. Mizutani, K. Wada and S. Kitagawa, *J. Am. Chem. Soc.*, 1999, **121**, 11425; (c) T. Kojima, T. Nakanishi, T. Honda, R. Harada, M. Shiro and S. Fukuzumi, *Eur. J. Inorg. Chem.*, 2009, 727.
49 (a) M. J. Crossley, P. L. Burn, S. S. Chew, F. B. Cuttance and I. A. Newsom, *J. Chem. Soc., Chem. Commun.*, 1991, 1564; (b) P. K. Kumar, P. Bhyrappa and B. Varghese, *Tetrahedron Lett.*, 2003, **44**, 4849.

This journal is © The Royal Society of Chemistry 20xx

Please do not adjust margins